2019 Mid-Atlantic Biomaterials Day Final Report

February 23, 2019

University of Maryland Society for Biomaterials Chapter
The Johns Hopkins University Society for Biomaterials Chapter

University of Maryland A. James Clark Hall, College Park, MD

Purpose:

The goal of this meeting was to gather individuals from academic institutions and businesses in the biomaterials field from the Mid-Atlantic region and beyond in order to provide a location such that innovation in the field of biomaterials can be shared amongst all attendees.

The meeting featured speakers involved with biomaterials work in academia, industry, and biotech entrepreneurship, networking sessions around meals, and a poster viewing session for students' research. We had multiple 15-minute breaks to also give all attendees the opportunity to talk with each other to spread ideas and knowledge between the different facets of professionals and students involved in biomaterials work. The topics of discussion ranged from research to the regulation and patenting process of the work.

Our goal for this event as to inspire and support the next generation of translational biomaterials scientists and engineers to innovate the next game-changing device or technology to benefit patients from debilitating disease. We emphasized that it's possible to actually benefit patients with technology that is developed at the bench. Sometimes that can be forgotten when working in the lab, so we wanted to drive that point through this meeting. Moveover, we wanted our attendees to realize that being a hardcore researcher isn't the only way to contribute to this goal. Additionally, we wanted to show our appreciation for all the students and acknowledge their research and contributions to the field of biomaterials.
Please see our list of speakers, affiliations and talk titles below.

Speakers:

Keynote

Chris Jewell, Ph.D., *University of Maryland, College Park*

"Harnessing biomaterials to study and control the immune system

Plenary

Emily English, Ph.D., *Gemstone Biotherapeutics*
"Beyond the Bench: Lessons Learned Transitioning a Research Project to a Product"

Stephen Horrigan, Ph.D. *Noble Life Sciences, Inc.*
"How to Convince other People to Use your Product"

Qijin Lu, Ph.D., *U.S. Food and Drug Administration*
"An Overview of Non-Clinical Hemocompatibility Evaluation of Blood-contacting Medical Devices and Biomaterials"

Hai-Quan Mao, Ph.D., *Johns Hopkins University*

“Injectable Nanofiber-Hydrogel Composite for Soft Tissue Regeneration”

Sean Virgile, MS, *Diagnostic anSERS Inc.*
“From the Bench to the *Road*side: Commercializing a Disruptive Technology”

Leah Kesselman, *Rheolution Inc.*
“Biomaterials Testing Breakthrough - from Bench to Booming Business”

Highlights:

There were many great talks throughout the day, but the talks by Drs. Christopher Jewell and Emily English surpassed our expectations. Dr. Jewell’s gave a more traditional research presentation that showcased his phenomenal research projects that investigate the interface between biomaterials and the immune system as the key to delivering therapies for many autoimmune diseases. Dr. English’s talk was a refreshing change of pace. She chose to highlight the logistics of translating a successful research project to a marketable product. She was able to use her experience as CEO of Gemstone Biotherapeutics as an example, which made her approach credible.

Success Story:

The 3rd annual Mid Atlantic Biomaterials Day was a huge success. Our attendance almost doubled from last years event with a total of about 60 people attending the event at the newly constructed Clark forum at the University of Maryland’s Clark Hall. Having industry relevant speakers seemed to make a large impact on the engagement from the crowd; The audience members asked a lot of questions after each talk and we often had to ask them to continue their dialogue at a later point in order to remain on schedule. We also witnessed many excellent posters and talks from undergraduate and graduate students alike. With such a wide range of experiences gathered under one roof, the event truly felt like a passing of the torch.

Photos:

Complete album can be here found here:
https://drive.google.com/drive/folders/1l1PijzmIeqSjE3BspoMZOrHm4N8U7JPO

Here are a few selected images


EXCELLENCE
EXCELLENCE
EXCELLENCE
EXCELLENCE

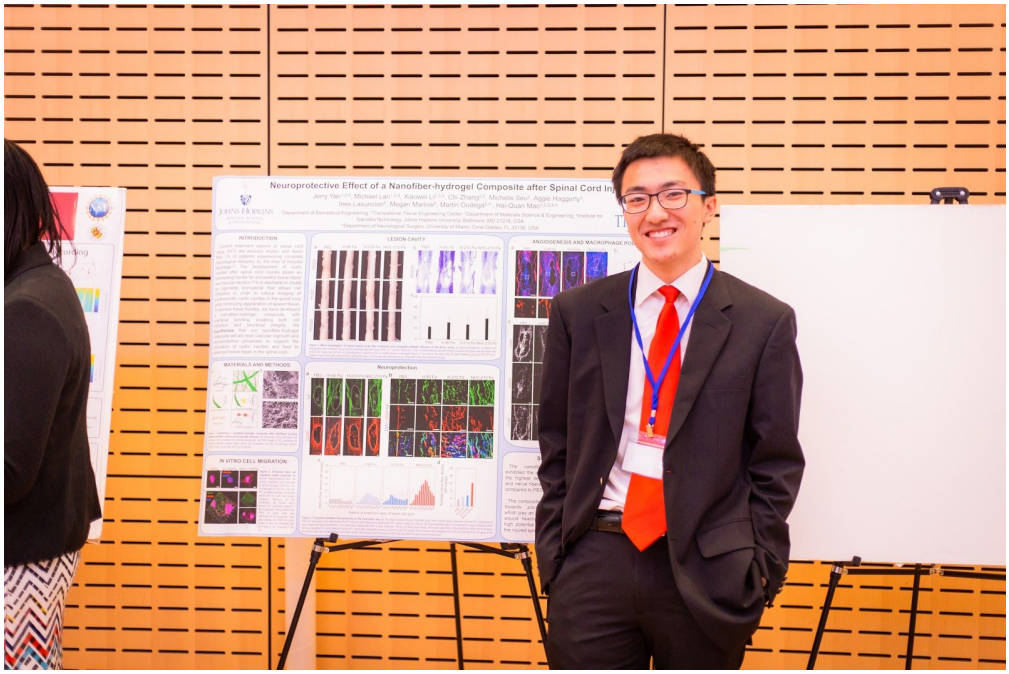
Neuroprotective Effect of a Nanofiber-hydrogel Composite after Spinal Cord
JOHNS HOPKINS
INTRODUCTION
LESION CAVITY
MATERIALS AND METHODS
Neuroprotection
IN VITRO CELL MIGRATION

Abstracts are below:

2019 Mid-Atlantic Biomaterials Day

February 23, 2019

Translational Biomaterials: Closing the Gap from Bench to Bedside

Saturday February 23rd, 2019

From 10 AM to 5 PM

University of Maryland, College Park

A. James Clark Hall

8278 Paint Branch Dr.,

College Park, MD 20740

We are now accepting abstracts for rapid fire talks and posters for the 3rd annual Mid-Atlantic Biomaterials Day!

To submit an abstract or register for tickets, visit: https://midatlanticbiomaterialsday2019.squarespace.com

Keynote Address

Dr. Chris Jewell –
University of Maryland , College Park

Speakers

Dr. Emily English – Gemstone Therapeutics
Dr. Stephen Horrigan – Noble Life Sciences
Dr. Qijin Lu – US FDA
Dr. Hai-Quan Mao – Johns Hopkins
Sean Virgile – Diagnostic anSERS Inc.
Leah Kesselman – Rheolution Inc.

Networking Opportunities!
Prizes for Best Research!
Catered Food!

Hosted by the SFB Chapters at University of Maryland and Johns Hopkins

Nanoparticle Multi-Drug Delivery Platform for the Treatment of Breast Cancer

Kisha Patel, Dr. Stephany Tzeng, Dr. Jordan Green
Johns Hopkins University Whiting School of Engineering, Johns Hopkins Medical Institute - Wilmer Eye Institute

Statement of Purpose: Breast cancer (BC) is the second leading cause of cancer related death in the United States. Every year there are over 200 thousand new cases of BC and approximately 40 thousand BC deaths annually in the United States alone. [1] BC is particularly deleterious because of its potential to metastasize and spread through the circulatory system. The key challenges in BC research are gaining the ability to selectively target tumor cells without harming healthy cells, improving the ease of application of the treatment, reducing the required frequency of the treatment, and personalizing treatments to suit the patients' individual needs, such as the stage of cancer development. In order to overcome these challenges, a systemic nanoparticle multidrug delivery system is required, which would allow for the administration of various therapeutic agents via a subcutaneous injection to facilitate a multifaceted treatment plan. The backbone of this platform relies on the Enhanced Permeability and Retention (EPR) effect which allows for increased accumulation and release of nanoparticles and agents at the tumor site. Anti-Hypoxia Inducing Factors (anti-HIF) agents will be use do decrease the ability of the tumor tissue to promote angiogenesis. Such agents include doxorubicin, acriflavine, and digoxin.[3] In order to increase the serum half-life of such therapeutic agents, we propose encapsulating each drug in nanoparticles made of a tri-block co-polymer of poly(lactic-co- glycolic acid) (PLGA) and poly(ethylene glycol) (PEG). PEG would increase the half-life by coating the nanoparticle, thus decreasing uptake by macrophages and other surveillance cells and PLGA would allow for a sustained release kinetics which allows for fewer individual doses to be administered.

Methods: PLGA is the primary polymer to be used because it is a component of many FDA-approved devices and applications and has been proven to have low immunogenicity.[2] Its hydrophobicity can be altered to alter release kinetics of the therapeutic agents therefore allowing increased freedom in optimization of a treatment regimen for patients with varying degrees of cancer progression. The nanoparticles are fabricated through a nanoprecipitation process in which the polymer is dissolved in a water-miscible solvent, such as DMSO, and the drug is dissolved in another water-miscible solvent, such as acetone, and they are mixed and added to an aqueous poly(vinylalcohol) (PVA) solution under sonication. These components are then placed on a stir plate for three hours for the particles to harden and the organic solvents to diffuse away or evaporate. The release of the drugs from the particles has also been studied and is important in understanding the length of time of effective treatment. The particles will be optimized to release for a two-week window. Cell studies have already been done to verify the biological effect of these therapeutic agents on HIF-1 signaling. After the optimization of the nanoparticle coating and dosage levels, they are injected via the tail vein into mice to better understand the biodistribution of the particles in the body. This can be done through the use of an In Vivo Imaging System (IVIS) and fluorescence measurements of blood samples taken at various time points from the treated mice. Because the particles are also loaded with Cy7.5 fluorescent dye, we will be able to track the circulation of the particles within the mouse body. The fluorescence of each major organ and tumor is analyzed in order to understand the accumulation of the nanoparticles in the body.

Results: The size of the fabricated nanoparticles was analyzed by dynamic light scattering (DLS). The optimal diameter of these particles is under 200 nm to prevent blockage in blood vessels and to exploit the EPR effect was reached. Biodistribution studies were also performed and showed upwards of 15% accumulation at the tumor site which is significant.

Conclusions: The nanoparticle synthesis process has been optimized and methods to increase targeted accumulation of particles are underway. In order to increase the longevity of the particles in the circulatory system, a red blood cell coating can also be added to avoid immune surveillance. In the future, the loading of digoxin, an anti-HIF agent, must be optimized. Digoxin is about a hundred-fold more potent than doxorubicin and acriflavine, therefore increasing the need to optimize its encapsulation efficacy.[3] Acriflavine biodistribution studies will also be essential in understanding how effective the treatment method is. This will be performed within upcoming months. All biodistribution studies will also have to be repeated with a larger sample size. Once biodistribution studies have been completed, the nanoparticles will be injected in varying combinations in order to optimize the treatment and the tumor regression will be tracked through IVIS imaging, protein assays to analyze HIF activity, etc.

References:

[1] Ma J., Jemal A. (2013) Breast Cancer Statistics. In: Ahmad A. (eds) Breast Cancer Metastasis and Drug Resistance. Springer, New York, NY.
[2] Jain R. (2000) The manufacturing techniques of various drug loaded biodegradable poly(lactide-*co*-glycolide) (PLGA) devices. Biomaterials. 21(23): 2475-2490.
[3] Zhang H. (2008) Digoxin and other cardiac glycosides inhibit HIF-1α synthesis and block tumor growth. PNAS. 105(50): 19579-19586.

Inkjet-Printed Scalable Electrocorticography Sensor

Alana Tillery[1], Jia Hu[2], Mathew Rynes[2], Suhasa B. Kodandaramaiah[2,3]
[1] Department of Bioengineering, University of Maryland, College Park, MD
[2] Department of Biomedical Engineering, University of Minnesota, Twin Cities, MN
[3] Department of Mechanical Engineering, University of Minnesota, Twin Cities, MN

Statement of Purpose: Brain-computer interfaces (BCI) have vast potential to augment and repair cognitive ability. Further, a class of BCI device which measures neural activity by flexibly conforming to the 3D topology of the brain is the electrocorticogram (ECoG) electrode array. Neural interfacing utilizing electrocorticography (ECoG) devices has been used to restore communication to individuals affected by late-stage amyotrophic lateral sclerosis [1] and to control a prosthetic limb [2]. In a minimally invasive manner, placement of ECoG arrays directly on the cortical surface avoids the diminished biocompatibility of implanting needle-like penetrating electrodes [3] while coupling high-resolution neural signal acquisition. The literature supports fabrication of an ECoG array requires microfabrication techniques, which can prove an insurmountable expense and barrier to entry into ECoG research [4]. To lessen the use of remote techniques, inkjet printing of conductive traces [5] and use of few microfabrication techniques has been published in the context of customizable, flexible neural interfaces [6]. In this work, we present a novel desktop ECoG array fabrication process entirely using commonly available desktop laboratory tools. We characterized arrays by conducting in vivo experiments in mouse models.

Methods: We began electrode array fabrication with 1) inkjet printing conductive electrode designs using silver nanoparticle (AgNP) ink on photo paper (Fig.2), as described in the literature [5]. To increase the biocompatibility and improve the neural signal acquisition of the AgNP traces, we 2) added a protective layer of the conductive biopolymer polyethylene dioxythiophene polystyrene sulfonate (PEDOT:PSS) [6] and sintered the AgNPs and PEDOT:PSS at 135°C. Through 3) coating the electrode traces between the rectangular pads and circular contacts with UV-curable polymethyl methacrylate (PMMA) and subsequent UV-treatment, we prevented interelectrode shorting and increased the durability and adhesion while maintaining the flexibility of the array. The durability of printed ECoG arrays was measured by a) mimicking neural conditions by immersing arrays in 1x phosphate-buffered saline (PBS) solution for five days as described previously [7] for a satisfactory electrochemical impedance of under 1 MΩ [3] at a sampling frequency of 1 kHz and b) adhering Scotch tape and a 200 g mass to the array as published previously as an adhesion test[8] and upon pull-off assessing endurance of the electrodes against delamination. To collect neural signals in vivo, we designed a custom 12-channel printed circuit board (PCB) with a molex connection and clamping mechanism to interface with an amplifier.

Results: Following five-day submergence in 1x PBS, electrode arrays had a range of impedances of 0.876 – 3.11 kΩ. After the Scotch tape adhesion test, arrays showed limited fracturing or discontinuities in Ag nano and PEDOT:PSS traces.

We conducted in vivo experiments with head-fixed mice anesthetized with isoflurane, yielding a range of electrode impedances of 2.42 – 3.11 kΩ. Using MATLAB to compute a short-time Fourier transform, we processed electrocorticograms and observed that the burst-suppression events, wherein a burst of voltage spikes from groups of neurons is suppressed as shown in Fig. 4 (red arrows), from our neural data were characteristic of the anesthetic employed and in agreement with prior studies [9].

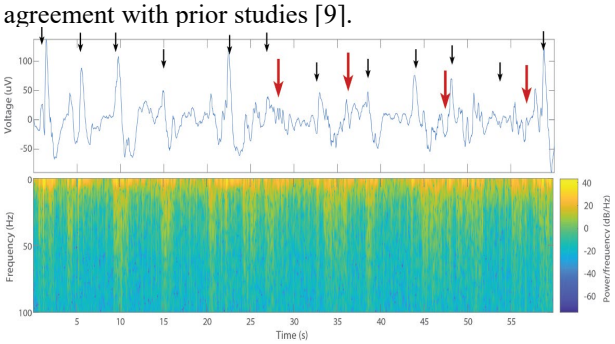

Figure 4: Processed voltage data from an acute anesthetized mouse experiment (black arrows: breathing artifacts, red arrows: burst-suppression).

Conclusion: A fabricated ECoG array (shown in Fig. 4) had a mass of 3 g, comparable to about 10% of the mass of a mouse. Arrays could be rapidly prototyped with a total production time of one hour and facilitate modularity and adaptability with existing ECoG array connection modalities. Moreover, the accessibility of the array provides a platform for single-use applications as would appear in medicinal research settings. We expect that this novel approach will facilitate high-level customizability, accessibility, and rapid prototyping of ECoG arrays that can be of use to the BCI community.

References: [1] Schnitker J. Adv Biosyst. 2018;2(3):1700136.

[2] Yanagisawa T. J Neurosurg. 2011;114(6):1715-1722.

[3] Ward M. Brain Res. 2009;1282:183-200. doi:10.1016/j.brainres.2009.05.052

[4] Toda H. Neuroimage. 2011;54(1):203-212.

[5] Kawahara Y. UbiComp 13. 2013.

[6] Kim Y. Sensors and Actuators B: Chemical. 2017;238:862-870.

[7] Dong S. Vacuum. 2017;140:96-100.

[8] Sridhar A. Thin Solid Films. 2009;517(16):4633-4637.

[9] Akrawi W. *J Neurosurg Anesthesiol*. 1996;8(1):40-46.

Jiaxiang Tao

Abstract

Human skeletal muscle is a dynamic biomaterial that provides the crucial mechanical support for our body. It undergoes rigorous self-repair after injury, due to the robust activation and self-renewal of muscle satellite cells, which consists of only 5% of all muscle cell types. Such amazing regenerative capability has significant biological and clinical values. Within the uninjured muscles, the mechanical property of skeletal muscle insures the relative stability of satellite cells, which live in an extremely compressive environment and are mostly quiescent. However, a muscle injury disrupts the "normal living environment" of satellite cells, bringing changes such as sudden increase in skeletal muscle stiffness and decrease in satellite cells' apical compressive pressure. These changes force the satellite cells to enter cell cycle and differentiate into myoblasts, which will then form the new muscle fibers and restore the damaged contractile functions within the myofibers. We consider cells that stably express Pax7 have such regenerative abilities, and they start to express MyoD when they are myogenic committed.

Here, we came up with possible mechanism and process of mechanosensitive activation and renewal of satellite cells by using the mouse model. We isolate muscle satellite cells from Pax7-ZSgreen mice's hindlimb using FACS and cultured them on Matrigel/Fibronectin-coated dish with different stiffnesses, with and without mechanical compression. This single-cell study gives us an insight in how human skeletal can maintain its relatively stable property throughout our life time.

Self-Assembled 3D DNA Crystals as Vehicles for Drug Delivery

Emily Luteran, Dr. Paul Paukstelis.
The University of Maryland, College Park.

Statement of Purpose: Deoxyribonucleic acid (DNA) is the storage material for genetic information, but has recently been repurposed as a building block in the construction of nanoscale assemblies[1]. The biocompatibility, stability, programmability, structural predictability, and ability to assemble into two- and three-dimensional (2 and 3D) structures[2] has made DNA a promising vehicle to aid in drug delivery applications. Therapeutics are typically delivered to patients in a non-specific manner, resulting in reduced overall efficacy and increased onset of side effects. As such, packaging and delivering therapeutics in a targeted, controlled manner would vastly improve treatment outcomes. The versatility of DNA assemblies makes them ideal candidates as vehicles for directed drug delivery in a promising effort to overcome this problem. This work specifically explores an entirely new platform for DNA-based drug delivery where self-assembled 3D DNA crystals are used to deliver cargo to cells.

Methods: This work uses a 13-nucleotide (13-mer) DNA that self-assembles in the presence of Mg^{2+} to form porous, high DNA density crystals with 2 nanometer solvent channels that run throughout the crystal[1]. These crystals are excellent candidates for use in drug delivery as therapeutic molecules can be incorporated into the solvent channels of the DNA crystal as well as via intercalation. This vastly increases the loading capacity of the container and allows for diversity in the type of drug that can be loaded or covalently attached to specific positions in the crystal lattice. In this work, the 13-mer crystals are treated with a chemical crosslinker (nornitrogen mustard; NOR) to enhance thermal stability and resistance to nuclease degradation in biological environments[3]. Following the crosslinking procedure, the crystals are loaded with the anti-cancer drug Doxorubicin (DOX). DOX incorporation is qualitatively evaluated by the visual identification of red coloration that is associated with the anthraquinone chromophore within DOX. The identification of the red coloration within the crystals is visualized using a Leica S8 APO Stereomicroscope. DOX leakage rates, and incorporation and release are evaluated using DOX fluorescence emission at 590 nm.

Results: To date, microscopy has been used to qualitatively evaluate the ability of wild-type (WT) and crosslinked (XL) 13-mer DNA crystals to incorporate and retain Doxorubicin. Crosslinked crystals were studied in parallel with WT crystals to observe improved crystal lattice stability during DOX loading. For DOX loading, the crystals (WT & XL) were soaked in various concentrations of DOX (0 uM, 100 uM, 250 uM, 500 uM) and stored at either 4°C or 22°C to allow DOX to incorporate into the crystal lattice via diffusion. The DOX exposed crystals were monitored for 7 days (Figure 1). Localization of red coloration within the WT and XL crystals was observed after 6 hrs.

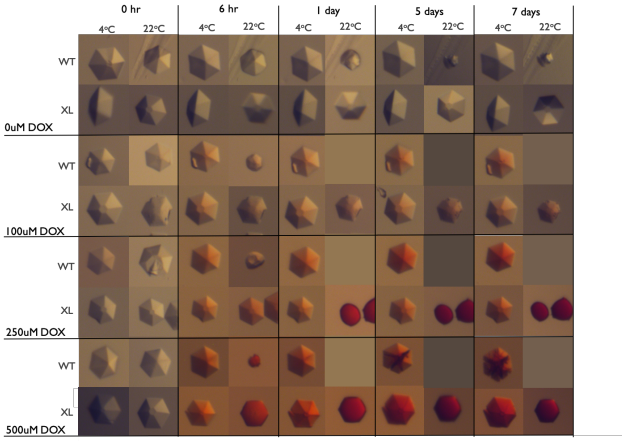

Figure 1. *DNA crystals loaded with DOX for 7 days.*

As DOX loading concentration increased, there was an associated increase in intensity of localized red coloration within the crystal. Similarly, as time progressed, the intensity of red coloration within the crystal increased. At 4°C and high DOX concentration, WT crystals began to fracture as a result of high DOX intercalation interrupting lattice stability. Alternatively, the integrity of XL crystals exposed to high DOX concentration at 4°C remained intact after 7 days of exposure. DOX loading was further evaluated at various concentrations of Mg^{2+}. As $[Mg^{2+}]$ was decreased, crystal lattice contacts are weakened and DOX intercalation via diffusion increased. After successful loading, crystals were transferred to fresh buffer solution to monitor leakage. At high DOX concentrations, XL crystals successfully retained DOX cargo for 24 hours. Loading capacity and leakage rates of DOX from crystal containers will be determined quantitatively with fluorescence spectroscopy.

Conclusions: This work illustrates the ability of doxorubicin, a small molecule anti-cancer drug, to be incorporated into a 3D DNA crystal. Upon exposure to high concentrations of DOX, crosslinked 13-mer DNA crystals retain structural integrity while localizing high quantities of drug within the crystal lattice. Exposure to high concentrations of DOX accompanied by low Mg^{2+} concentrations result in intense red coloration, DOX, localized within the crystals. This preliminary work shows that DNA crystals can load and retain DOX, which further indicates that technology has the potential to be further developed as a vehicle for targeted drug delivery.

References:

1. Paukstelis PJ. Chem Biol. 2004;11:1119-1126.
2. Paukstelis PJ. Crystals. 2016;6:97.
3. Zhang, D. ChemBioChem. 2016;17:1163-1170.

Development of a novel 3D bioprinting method using a Poly-L-Lysine based hydrogel scaffold

Narendra Pandala[1], Adam Day[1], Erin Lavik[1].
[1]Department of Chemical, Biochemical and Environmental Engineering, University of Maryland, Baltimore County.

Statement of Purpose: *In vitro* models provide a good starting point for drug screening and understanding various cellular mechanisms corresponding to different conditions. Even though conventional 2D cell cultures been useful in providing valuable information, a monolayer of cells lacks some physiological characteristics exhibited by the cells *in vivo*. To better mimic the in vivo microenvironment, and to overcome the limitations of the 2D monolayered cultures 3D cultures are used. 3D bioprinting techniques have recently emerged as a useful tool which print cells into different tissue structure providing a potential alternative as 3D cultures in developing drug screens and various tissue engineering applications. Even though 3D bioprinting serves as very useful tool, it is highly expensive and comes with a few limitations. For example, the bio ink used in the printers has viscosity limitations which in turn effects the shapes and structures to be printed, and also the cells undergo temperature changes and sheer stress which effects their viability. The electronics industry uses screen printing in order to print layers of conductive and resistive materials onto printed circuit boards [PCB]. Taking cues from this we have developed a screen printing process which prints layers of bio ink which is composed of a hydrogel scaffold and the cells, on to different surfaces and grow them in a 3D culture. The screen printing process is not only very cost effective (does not require expensive specialized equipment) but also can be used to print patterns with a fine resolution to scale of micrometers. Also, this process can be used to print repeated patterns of layers of the cells and constructing multilamellar structures, which makes it potentially a very good alternative technique for 3D bio printing. This poster presents the synthesis, characterization and mechanical testing of a polyethylene glycol (PEG) – poly-l-lysine (PLL) based hydrogel to be used as a bioink in the screen printing process. Also, this poster shows the effect of screen printing process on the viability of the cells.

Methods: A hydrogel composed of poly-l-lysine(PLL) functionalized by vinyl sulfone(VS) is crosslinked with di thiol PEG (SH-PEG-SH) to be used as the scaffold in the printing process. In the first step of the synthesis of the VS-PEG-PLL macromer, the di hydroxyl PEG (OH-PEG-OH) is attached to poly-l-lysine by using carbonyldiimidazole (CDI) chemistry. In the next step, vinyl sulfone groups are attached to the PEG-PLL obtained in the first step using one step click chemistry to form the VS-PEG-PLL macromer. In each step of the synthesis the compound formed is characterized by using NMR spectroscopy and OPA assay. The elastic, viscoelastic moduli and gelation time results of the synthesized hydrogel were obtained using a Stress Control Rotational Shear Rheometer. Using Gelatin as an analogue to the hydrogel, human Colorectal adenocarcinoma cells (Caco-2) were printed using the screen printing process along with appropriate controls in order to measure the effect of the screen printing process on the viability of the cells.

Results and Discussion: NMR spectra of the confirms the presence of the synthesized macromer. The rheometric data gives an elastic modulus of 108 Pa with a gelation time of 15 minutes, which is in the workable range of the screen printing process. The live dead data shows that the screen printing process results has a survival rate of 80% (Figure -1) This is promising and comparable to that of a 3D bioprinter and much lower cost

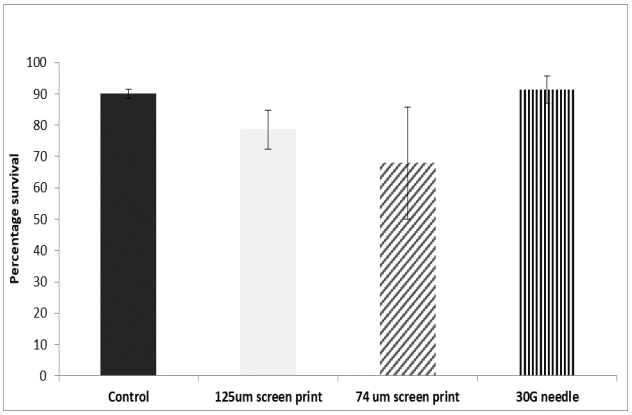

Figure 1 : Viabilities of Caco-2 cells through the screen printing process using a gelatin analog

Engineering ClpS For Selective And Enhanced N-terminal Amino Acid Binding To Tyrosine

Emily Samuels [2,3], Kunal Dharmadhikari [2,3], Makenzie Christensen[2], Jennifer Tullman [1,2], Christina Bergonzo [1,2], Zvi Kelman [1,2], and John Marino [1, 2]

[1] Biomolecular Measurement Division, National Institute of Standards and Technology, Gaithersburg, MD 20899

[2] Biomolecular Structure and Function Group, Institute for Bioscience and Biotechnology Research Rockville, MD 20850

[3]University of Maryland, College Park, MD 20742

Statement of Purpose: Achieving high-fidelity, sequential recognition and detection of specific amino acids that comprise the peptide sequence is a challenge in the development of single-molecule protein sequencing technologies[1]. An approach to achieve this goal would be to amplify naturally occurring proteins that function through recognition of amino (N)-terminal amino acids (NAAs). One of these proteins is the N-End Rule Pathway adaptor protein ClpS[2,3]. The native ClpS protein has a high specificity yet modest affinity for the amino acid Phe at the N-terminus but also recognizes the residues Trp, Tyr, and Leu at the N-terminal position[1]. In this study, we have used molecular dynamic simulations to select for ClpS variants with enhanced affinity and selectivity for an NAA (Tyr). Using this approach, two variants of the *Agrobacterium tumefaciens* ClpS protein with different mutations at specific native residues. A third variant was identified using the PROSS algorithm and predicted to help stabilize the protein without affecting the binding pocket[4]. We are currently using in vitro surface binding assays, such as yeast display, to test these variants of the ClpS protein through a combination of these mutations for tighter binding to tyrosine.

Methods: A combination of suggested mutations from the molecular dynamics simulations and the PROSS algorithm were cloned into the pCTCON2 vector. To clone the targets into this vector, the DNA for the ClpS mutant proteins were PCR amplified and digested at the NheI and BamHI sites. This insert was then ligated into the pCTCON2 vector at those sites. The ligated sample was transformed into DH5a *E. coli* for plasmid extraction and sequencing confirmation. Once the samples were confirmed, they were transformed into yeast to determine binding activity. A fluorescent labeling scheme was used for detection of peptide binding in yeast during flow cytometry. The myc tag on the variant is detected with an AlexaFluor 647 labeled anti-myc antibody. The peptide is detected using streptavidin-PE which binds the biotinylated C-terminus of each peptide. The increased fluorescence of both the AF647 and SA-PE in quadrant 2 of the flow cytometry results indicated enhanced binding affinity of the protein to the peptide.

Results: We used the fluorescent labeling technique on WT, PROSS, L9N and L9N PROSS mutants with varying concentrations of the peptides tyrosine (Y) and phenylalanine (F) from 0.1 uM -10uM. The WT ClpS protein had a PE fluorescence of 5E6, PROSS had 5E6, L9N had 5E6 L9N PROSS mutant had a PE fluorescence of 2E7 at a tyrosine concentration of 5uM. The PROSS mutation stabilizes and improves binding as well as the L9N which increases H bonding. So a combination of these two mutations has a significant increase in the N-terminal binding to tyrosine compared to the WT protein.

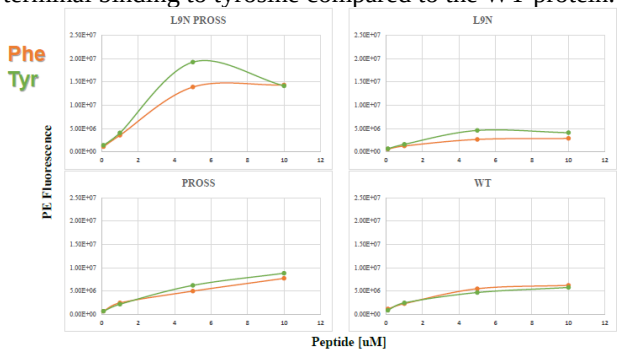

Figure 1. Experimental yeast assays, fluorescence traces Fluorescence traces from flow cytometry shown for the L9N and L9N PROSS variants in the presence of varying concentrations of the peptide phenylalanine and tyrosine.

Conclusions: From the yeast display assay, the variants of the ClpS protein that had enhanced tyrosine binding were L9N and L9N PROSS. A combination of simulation methods and experimental evidence confirms the usefulness of the L9N mutation for binding N-terminal tyrosine. We can approach the binding site design for other N-terminal residues by optimizing hydrophobic packing to potentially provide insight for peptide sequencing. And to recognize charged amino acids we will need to identify a different protein.

References:

1. Stein BJ, Grant RA, Sauer RT, Baker TA (2016) Structural Basis of an N-Degron Adaptor with More Stringent Specificity. Structure 24:232–242 . doi: 10.1016/j.str.2015.12.008

2. Ahyoung AP, Koehl A, Vizcarra CL, Cascio D, Egea PF (2016) Structure of a putative ClpS N-end rule adaptor protein from the malaria pathogen Plasmodium falciparum. Protein Sci 25:689–701. doi: 10.1002/pro.2868

3. Erbse A, Schmidt R, Bornemann T, Schneider-Mergener J, Mogk A, Zahn R, Dougan DA, Bukau B (2006) ClpS is an essential component of the N-end rule pathway in Escherichia coli. Nature 439:753–756 . doi: 10.1038/nature04412

4. Campeotto, I.; Goldenzweig, A.; Davey, J.; Barfod, L.; Marshall, J. M.; Silk, S. E.; Wright, K. E.; Draper, S. J.; Higgins, M. K.; Fleishman, S. J. One-Step Design of a Stable Variant of the Malaria Invasion Protein RH5 for Use as a Vaccine Immunogen. Proc. Natl. Acad. Sci. U. S. A. 2017, 114 (5), 998–1002.
PMID: 28096331 DOI: http://dx.doi.org/10.1073/pnas.1616903114

Isolation and Decellularization of Porcine Urinary Bladder Matrix for Extracellular Matrix-Based Wound Dressing Applications

Jules Allbritton-King[1,2], Megan Kimicata[2,3], JP Fisher[1,2]
[1]Fischell Department of Bioengineering, University of Maryland, College Park MD
[2]Center for Engineering Complex Tissues, University of Maryland, College Park, MD
[3]Department of Materials Science and Engineering, University of Maryland, College Park, MD

Statement of Purpose: Extracellular matrix (ECM) is the network of proteins and other macromolecules that support and anchor cells within tissue. Porcine urinary bladder matrix (UBM) has been previously used as a biomaterial for wound dressings due to its strength and compliance.[1,2] The objective of this work is to isolate and decellularize porcine UBM without disrupting native ECM components for future development into an ECM-based hydrogel wound dressing. A hydrogel dressing will provide a physiologically relevant moisture balance and mimic the mechanical properties of native dermis. The extent of decellularization was assessed by the widely accepted threshold of <50ng DNA per mg dry tissue to minimize immunogenic response upon implantation. [3]

Methods: Whole porcine bladders (Animal Biotech) were distended with PBS overnight to loosen the bladder's muscle fibers. The bladders were then dissected and the luminal bladder ECM (LB-ECM) was mechanically delaminated. LB-ECM refers to UBM and any other tissue layers that remained attached during the delamination process, as the specific tissue layers delaminated from the whole bladders have not yet been histologically confirmed. Samples of LB-ECM were decellularized using a protocol adapted from Gui et. al.[4] The DNA content of native and decellularized LB-ECM was assessed quantitatively via Picogreen assay, and qualitatively via DAPI nuclear staining. Protein content of LB-ECM samples before and after decellularization was assessed with SDS-PAGE to ensure minimal disruption to native ECM proteins.

Results: LB-ECM decellularized as described above was found to have an average of 20.4(±3.2) ng DNA/mg dry tissue, corresponding to >99.5% DNA reduction from native LB-ECM (Figure 1A). Qualitatively, there were no visible nuclei remaining in decellularized LB-ECM samples following DAPI staining (Figure 1B). Electrophoresed samples of LB-ECM confirmed a large component of collagen type I in both native and decellularized tissue (Figure 1C). Some low molecular-weight banding was noticeably fainter for decellularized LB-ECM, but otherwise the protein content of decellularized LB-ECM remained largely unchanged from that of native LB-ECM. Future experimentation will assess the retention and modification of other major ECM components, such as glycosaminoglycans (GAGs).

Conclusions: Distention of the bladder prior to dissection minimized retention of other non-UBM tissues during delamination, given the extent to which native DNA was removed during the decellularization procedure. The decellularization process significantly reduced native DNA content of LB-ECM, despite limiting the tissue's exposure to "harsher" decellularization reagents such as SDS.[3,4] Furthermore, the protein content of the isolated LB-ECM was largely unaltered during decellularization. Retaining a high degree of similarity to native ECM is necessary to optimize cell adhesion and recruitment into the wound bed as per the body's natural wound healing response. These findings are important for future studies focusing on development of decellularized LB-ECM into a hydrogel and functionalization of the matrix components retained in the ECM.

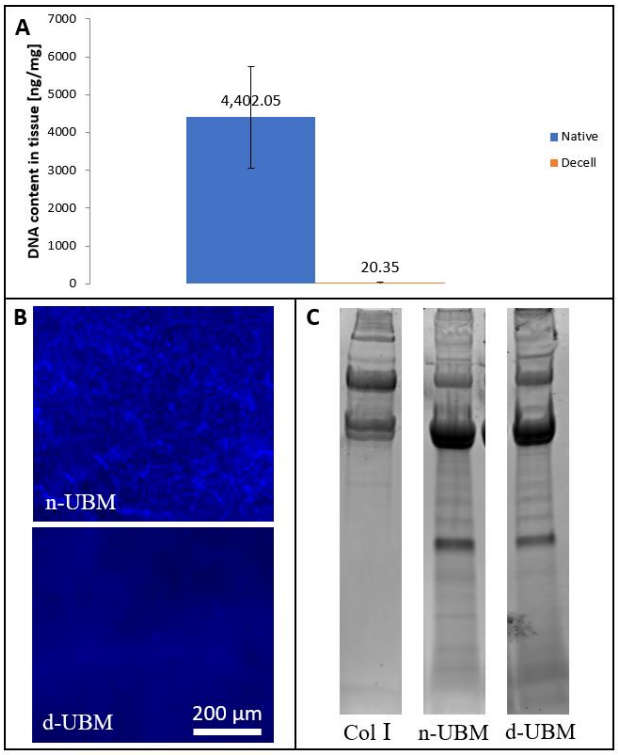

Figure 1: (A) DNA content of native and decellularized UBM, expressed in ng DNA per mg dry tissue. (B) DAPI nuclear stain imaging of native vs. decellularized UBM. (C) Electrophoresed protein gel images for a collagen I standard, native UBM, and decellularized UBM, respectively.

References:

1: Freytes, D. O. Biomaterials, 2008; 29(11), 1630–1637.
2: Rosario, D. J. Regenerative Medicine 2008; 3(2), 145–156.
3: Crapo, P. M. Biomaterials, 2011; 32(12), 3233-43.
4: Gui, L. Tissue Engineering Part C: Methods, 2010;16(2), 173–184.

Neuroprotective Effect of a Nanofiber-hydrogel Composite after Spinal Cord Injury

Jerry Yan[1, 4], Michael Lan[1,4], Xiaowei Li[1-3], Chi Zhang[1, 2], Michelle Seu[1], Yohshiro Nitobe[5], Kentaro Yamane[5], Aggie Haggerty[5], Ines Lasuncion[5], Megan Marlow[5], Martin Oudega[5-7 *], Hai-Quan Mao[1-4 *]

[1]Translational Tissue Engineering Center, [2]Department of Materials Science & Engineering, [3]Institute for NanoBioTechnology, [4]Department of Biomedical Engineering, Johns Hopkins University, Baltimore, MD 21218, [5]The Miami Project to Cure Paralysis, [6]Department of Neurological Surgery, University of Miami, Miami, FL 33136, [7]Bruce W. Carter Department of Veterans Affairs Medical Center, Miami, FL 33136, USA. *Corresponding authors.

Statement of Purpose: Contusion is the prevalent mechanism of spinal cord injury (SCI) in humans. The efficacy of available therapies for spinal cord contusion is limited, with less than 1% of the patients experiencing complete neurological recovery by the time of hospital discharge. [1] Contusions cause loss of nervous tissue and ultimately the formation of cystic cavities at the injury site, which poses a formidable obstacle for tissue repair and functional recovery. [2] Creating a favorable environment for nervous tissue sparing and regeneration may support improved functional outcomes. We have developed an injectable nanofiber-hydrogel composite (NHC) with interfacial bonding that enables cell infiltration while providing structural integrity for bridging cystic cavities in the injured spinal cord. The purpose of this work was to evaluate the effects and potential mechanisms of NHC on neuroprotection in an adult rat model of spinal cord contusion.

Materials and Methods: To develop the nanofiber-hydrogel composite, we functionalized polycaprolactone fibers with maleimide groups and conjugated them to a thiol-modified hyaluronic acid hydrogel matrix through Michael-type addition chemistry. For the spinal cord contusion, the eighth thoracic (T8) vertebra of the spinal cord in adult Sprague-Dawley rats was exposed and then impacted at 175 kDyne using the Infinite Horizon Impactor. Three days later, the contused T8 was injected with PBS, 80-Pa hydrogel (H-80 Pa), 210-Pa hydrogel (H-210 Pa), or 210-Pa nanofiber-hydrogel composite (NHC-210 Pa; Hydrogel phase: 80-Pa). At defined time points after the injection, the rats were perfused with 4% paraformaldehyde. Then the spinal cords were resected and processed to determine the amount of spared nervous tissue in the contused T8 segment. Immunohistochemistry was performed to identify blood vessels, reactive astrocytes, neurons, axons, and macrophages at the contusion site, all of which were quantitatively analyzed using ImageJ software.

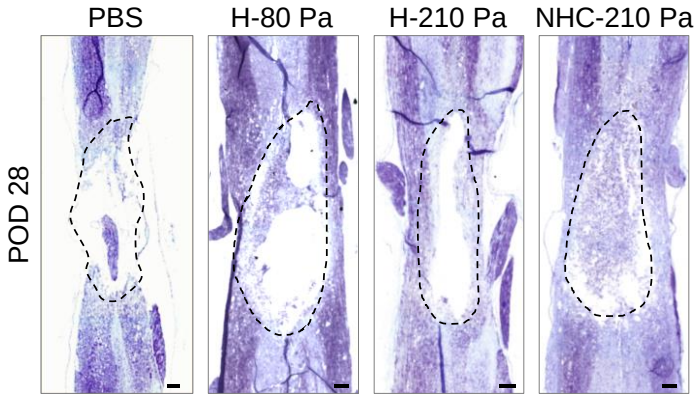

Figure 1. Nissl staining was performed on T8 segment for each treatment group at post treatment-operation day (POD) 28 in order to observe and quantify the size of lesion cavity. Scale = 200 μm. The lesion cavity percentage (7.4%) is the smallest for the NHC treatment group. Multiple layers of sections from each group were used to create a 3D reconstruction of the lesion cavity using the lesion areas present to calculate the volume as a percentage of the whole spinal cord section.

Results and Discussion: Gross anatomical evaluation of the contused spinal cords suggested less damage over time at the injury epicenter with the treatment of NHC compared with hydrogels and PBS. Preliminary histological data confirmed decreased tissue loss in contused segments following injection of NHC, especially when compared to other treatments (**Fig. 1**). Furthermore, injection of NHC resulted in the highest densities of blood vessels and axons within the contusion site (**Fig. 2**). The number of inflammatory cells at the contusion site appeared similar among all experimental groups. However, compared to other treatment groups, NHC-treated spinal cord presented the most pro-regenerative M2 macrophage phenotypes (Data not shown).

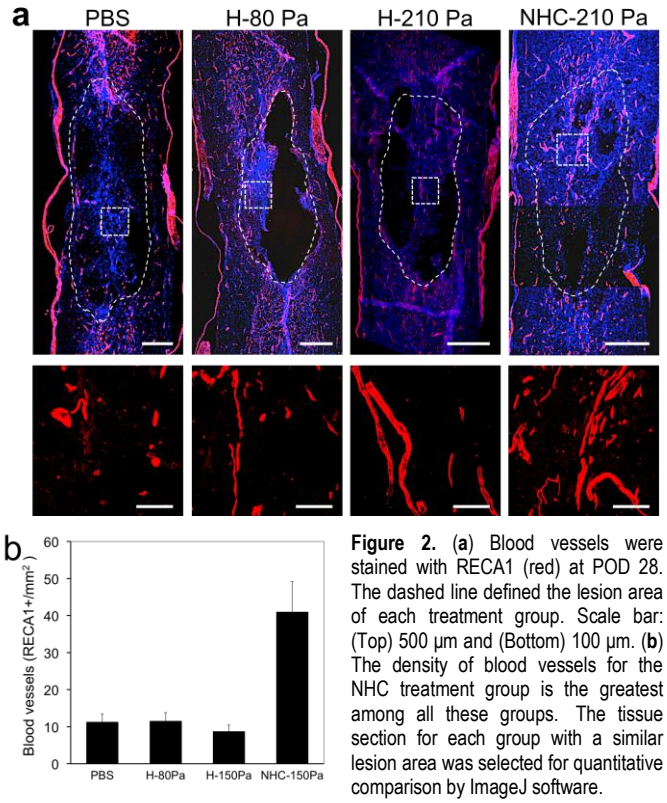

Figure 2. (**a**) Blood vessels were stained with RECA1 (red) at POD 28. The dashed line defined the lesion area of each treatment group. Scale bar: (Top) 500 μm and (Bottom) 100 μm. (**b**) The density of blood vessels for the NHC treatment group is the greatest among all these groups. The tissue section for each group with a similar lesion area was selected for quantitative comparison by ImageJ software.

Conclusion: We developed a unique injectable nanofiber-hydrogel composite for supporting repair of the contused spinal cord. Our results suggest that angiogenesis and immunomodulation are possible mechanisms underlying neuroprotection and axon growth in spinal cord lesions.

References:

1. National Spinal Cord Injury Statistical Center, Facts and Figures at a Glance. Birmingham, AL: University of Alabama at Birmingham, 2017.

2. Hong, A *et al*. An Injectable Hydrogel Enhances Tissue Repair after Spinal Cord Injury by Promoting Extracellular Matrix Remodeling. *Nature Communications*, 2017, 8(1): 1-14.

Digging for Discoidin and Controlled Extracellular Vesicle Release

Chris Kuffner, Anjana Jeyaram, Eli Pottash, Steven Jay.
University of Maryland Department of Bioengineering

Statement of Purpose: Extracellular Vesicles (EVs) have emerged as a key mediator in the efficacy of cell therapies, but they rapidly clear from injection sites. This decreases efficacy of directly administered EVs relative to continuously secreted EVs from implanted stem cells. Recent studies have addressed this by trapping EVs in hydrogels for extended release [1,2].

In our research, we are engineering an EV binding protein to attach EVs to hydrogels. We aim to allow increased temporal and spatial control of delivery. The engineered protein uses a discoidin domain from lactadherin to bind phosphatidylserine on the surface of EVs[3]. We also explore this protein's interactions with hydrogel polymers.

Methods: A fusion protein was expressed on the pcDNA5 backbone with the EXPI293 mammalian expression system. The protein contains an azurocidin signal peptide for secretion on its N-terminus followed by GST, GFP, and the lactadherin C1C2 binding domain. Cells were transfected as per manufacturer's protocol, but were incubated until viability began to decline and cells started to clump at the bottom of their flask. Dead cells contain exposed phosphatidylserine that the C1C2 domain binds [4]. The clumps were isolated by skimming media away. Protein was isolated from clumps by adding MLBII lysis buffer (50 mM NaPO4, 300 mM NaCl, 0.5% Tween, pH 8) and incubating on ice[5]. Protein was purified using Genscript glutathione resin. Protein binding to EVs was tested by incubating HEK EVs in purified protein solution for 30 minutes at room temperature, then passing the solution through a 300kDa filter. Protein binding to collagen was tested in a similar manner using Cultrex Rat Collagen 1, which is 300kDa in solution.

The protein was also expressed in E. coli BL21 DE3 cells on a pET backbone without a secretion peptide. Protein was obtained from cell pellet by B-PER lysis then purified and tested as described above.

Results: Green fluorescence from eGFP in the protein was not substantially different in the cell pellet and media of transfected and untransfected cultures. However, clumps of dead cells at in each flask had substantially higher fluorescence in transfected culture (fig 1).

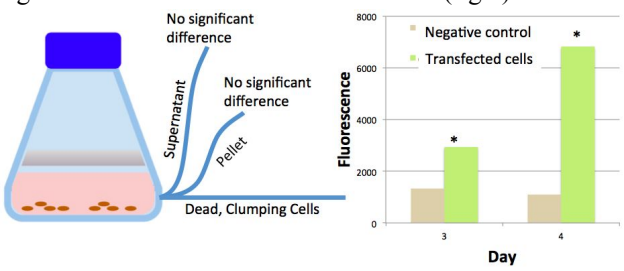

Figure 1. Green fluorescence of cell culture samples for transfected and control cultures. Clumps did not appear until day 3 post transfection. Green Fluorescence of clumps increased from days 3 to 4, concurrent with decreasing cell viability and increasing clump size.

A 92 kda band eluted from GST purification of clumping cells. The purified protein was confirmed to contain GFP and GST by western blot. Pure protein passed through a 300kDa filter, but the same protein did not pass when incubated with EVs (fig 2). These results were repeated and duplicated with bacterial-derived protein.

Figure 2. EV-binding prevents purified protein (E1) from passing a 300kDa filter column. ALIX antibody used for EV detection and GFP antibody used for purified protein detection.

When combined with rat collagen I, the protein did not pass through a 300kDa filter. Lower concentrations of collagen appear to produce darker bands of bound protein on a western blot.

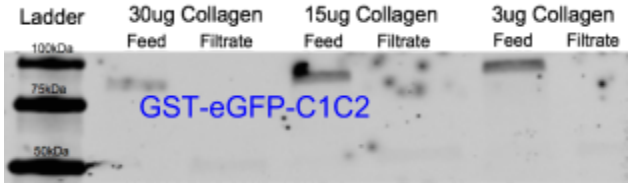

Figure 3. Protein will not pass through a 300kDa column in the presence of collagen. GFP antibody was used for protein detection.

Conclusions: We successfully expressed and purified fluorescent EV-binding protein from mammalian cells and e. Coli. The protein effectively bound to EVs, suggesting that it can be employed as a modular method to modify the EV surface. Preliminary results show that the protein binds collagen. Further testing is necessary to find a gel that will not interact with the protein in unpredictable ways as seen in the results. Continuing studies will investigate applications of this protein for gel-based controlled delivery of extracellular vesicles. This research may present an improved alternative to stem cell therapies by more effectively replicating cellular release of extracellular vesicles.

References:

1. Liu, B., Lee, B. W., Nakanishi, K., Villasante, A., Williamson, R., Metz, J., Kim, J., Kanai, M., Bi, L., Brown, K., Di Paolo, G., Homma, S., Sims, P. A., Topkara, V. K., … Vunjak-Novakovic, G. (2018). Cardiac recovery via extended cell-free delivery of extracellular vesicles secreted by cardiomyocytes derived from induced pluripotent stem cells. *Nature biomedical engineering*, *2*(5), 293-303.
2. Zhang K., ZhaoX., Chen X., Wei Y., Du W., Wang Y., Liu L., Zhao W., Han Z., Kong D., Zhao Q., Guo z., Han Z., Liu N., Ma F., Li Z. (2018). Enhanced Therapeutic Effects of Mesenchymal Stem Cell-Derived Exosomes with an Injectable Hydrogel for Hindlimb Ischemia Treatment. *ACS Applied Materials & Interfaces*, *10(36)*, 30081-30091
3. Jialan S., Christian W. H., Jan T. R., Gary E. G., (2004). Lactadherin binds selectively to membranes containing phosphatidyl-l-serine and increased curvature. *Biochimica et Biophysica Acta (BBA) - Biomembranes*, 1669(1), 82-90.
4. Hankins, H. M., Baldridge, R. D., Xu, P., & Graham, T. R. (2014). Role of flippases, scramblases and transfer proteins in phosphatidylserine subcellular distribution. *Traffic (Copenhagen, Denmark)*, *16*(1), 35-47.
5. Wang, Jing-Hung, et al. (2018). Anti-HER2 ScFv-Directed Extracellular Vesicle-Mediated MRNA-Based Gene Delivery Inhibits Growth of HER2-Positive Human Breast Tumor Xenografts by Prodrug Activation. *Mol Cancer Ther; 17(5); 1133–42.*

Tolerogenic cargo delivery via polymeric microparticles in reducing autoimmune-specific inflammation

Maeesha Noshin[1], Emily Gosselin[1], and Christopher M Jewell[1-3]

[1]Fischell Department of Bioengineering, University of Maryland, College Park MD; [2]United States Department of Veteran Affairs, Baltimore MD, [3]Robert E. Fischell Institute for Biomedical Devices, College Park MD.

Statement of Purpose: Multiple sclerosis (MS) is an autoimmune disease in which the immune system attacks myelin, the matrix that insulates neurons. Immunosuppressants, the current form of treatment, are non-curative and broadly-acting, leaving patients immunocompromised. New therapeutics seek selective tolerance, specific to myelin primary and spread epitopes, by inducing regulatory T cells (T_{REGS}) that control disease. Microparticles (MPs) synthesized with the polymer poly(lactic-co-glycolic acid)(PLGA) are an ideal mechanism for delivering cargo to the lymph node (LN) microenvironment via intra-lymph node injections[1, 2]. MPs are large enough to resist drainage from LNs, providing myelin specific immune cells with longer-term exposure to cargo that can bias them toward regulatory phenotypes. We have previously shown that intra-LN (i.LN.) injection of biodegradable MPs that release myelin peptide and rapamycin (Rapa), a regulatory signal, can reprogram LNs to promote T_{REGS} in a progressive mouse model of MS [3]. Treatment with myelin oligodendrocyte glycoprotein (MOG) and rapamycin (Rapa), an immunomodulatory drug, have shown to restrain inflammatory cytokine secretion in in vitro models and as treatment in vivo in a model of RR-MS (RR-EAE), in which the immune system attacks multiple segments of PLP[3]. We hypothesize that co-delivery of myelin peptides PLP139-151 (primary epitope) and PLP178-191 (spread epitope) via MP treatment can reduce inflammatory cytokine secretion among splenocytes processed from mice induced with RR-EAE.

Methods: Poly(lactide-co-glycolide) MPs loaded with Rapa and/or myelin peptides – PLP139-151 and PLP178-191 – were prepared by double emulsion. Rapa loading was measured by UV-Vis spectrophotometry, and peptide loading was quantified using a microBCA Protein Assay. To test the inflammatory response to MPs treatment, whole splenocytes were collected from mice induced with RR-EAE and euthanized at D15 (peak of first wave of disease) and D61 (weeks after relapse). Splenocytes were plated into 96 well plates and then were either left unstimulated, or stimulated with soluble PLP139 or PLP178. Cells were then treated with 5 ug of MPs. The cells were incubated for 3 days followed by supernatant extraction and INF-γ ELISA to quantify concentrations of inflammatory cytokine release within each treatment group.

Results: Immune cells from mice spleens (splenocytes) that were treated with Rapa-loaded MPs secreted less INF-γ. Cells processed on Day 15 of RR-EAE – the peak of the first wave of disease – showed no reactivity to the epitope PLP178-191, but produced high amounts of INF- γ when exposed to PLP139-151. Some inflammatory response to PLP178-191 was present from cells at Day 61 of RR-EAE, in addition to high reactivity to PLP139-151. Down-regulation of INF- γ was unchanged between Rapa MPs treatment from Day 15 and Day 61.

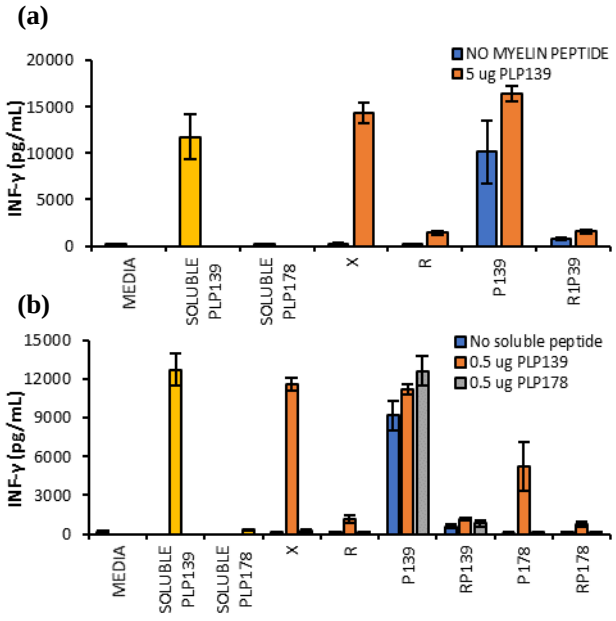

Treatment Key: **X** = Empty MPs, **R** = Rapa MPs, **P139** = PLP139-151 MPs, **RP139** = Rapa+PLP139-151 MPs, **P178** = PLP178-191 MPs, **RP178** = Rapa+PLP178-191 MPs

Figure 1. (a) Splenocytes isolated and treated on Day 15 of RR-EAE exhibit significant downregulation of INF-γ after treatment with Rapa. In accordance with first wave peak disease day, increased reactivity to epitope PLP139-151 follows. **(b)** This down-regulation of IFN-γ secretion was also shown in cells given MPs treatments containing Rapa at Day 61.

Conclusions: As a therapeutic to RR-MS, tolerogenic MP treatment successfully reduced inflammation. Signal stimulation from exposure to encephalitogenic epitopes are indicative responses of engineered specificity in this vaccine prototype. The key next steps are to study disease evolution and immune cell response to MPs over additional critical timepoints of RR-EAE. Understanding treatment response will require quantifying inflammation, T_{REG} proliferation and myelin-specific tolerance. This knowledge could advance future designs of disease-specific immunotherapies for translation to clinical use.

References:

[1] D.R. Getts, A.J. Martin, D.P. McCarthy, et al. Nat Biotechnol 30(12) (2012) 1217-24.

[2] M.L. Bookstaver, S.J. Tsai, J.S. Bromberg, C.M. Jewell. Trends Immunol 39(2) (2018) 135-150.

[3] L.H. Tostanoski, Y.C. Chiu, J.M. Gammon, et al. Cell Rep 16(11) (2016) 2940-2952.

Controlling zeta-potential of nanoparticles through surface modification to minimize complement activation in the immune system

Nuzhat Maisha*, Tobias Coombs* and Dr. Erin Lavik*

Department of Chemical, Biochemical and Environmental Engineering, University of Maryland Baltimore County

Statement of Purpose: While nanomedicines and protein-based drugs can be used for targeted drug delivery, these can trigger the complement pathway in immune system, leading to a pseudo-allergic reaction, involving major organs of the body due to anaphylatoxins produced. The anaphylatoxins (C3a, C4a and C5a protein fragments) are produced as the complement protein C3 encounters a foreign agent and deposits on it. A cascade of reactions is set in motion producing complement protein fragments C3a and C3b, leading to formation of complexes that produce C4a and C5a fragments, and these proteins work towards clearing the foreign agents from the system. This alters the biodistribution of the therapeutic. Moreover, complement protein fragments activate mast cells and neutrophils which can cause vasodilation, leading to excessive bleeding. The objective of this study is to determine the changes in complement protein levels in blood through in vitro ELISA assays when incubated with nanoparticles of different zeta potentials. Zeta-potential, a parameter closely related to particle charge is used to control complement activation. Previous study in porcine trauma model has shown lower complement activation related pseudo-allergy symptoms for nanoparticles having neutral zeta-potential. To form neutral nanoparticles, poly (L-lactic acid)-block-poly (ethylene glycol) (PLA-PEG) block copolymer containing amine end group was synthesized through ring opening polymerization based on Connor et al (Connor, Nyce, Myers, Möck, & Hedrick, 2002). We have successfully fabricated nanoparticles of different charges from various blends of PLA-PEG with and without amine groups, and then incubated the nanoparticles in blood, and quantified the changes in complement protein C5a level, which is a major anaphylatoxin in the complement activation cascade.

Methods: Poly (L-lactic acid)-block-poly (ethylene glycol) block copolymer and poly (d-lactic acid) polymer were synthesized through ring opening polymerization. Nanoparticles were formed by blending the polymers through nanoprecipitation starting with a polymer solution of concentration 20mg/ml. The nanoparticles were then incubated with human whole blood and plasma for 45 minutes at 37°C, and then C5a ELISA assay was performed to quantify changes in C5a level.

Results: The fold change in human whole blood was determined to be least in the sample incubated with neutral nanoparticle having zeta potential of -1.80 mV. As negative control, zymosan, a known complement activator was used. Samples incubated with zymosan showed more than 20-fold change in C5a level. Also, compared to plasma, whole blood was found to be more sensitive to changes in complement protein levels. One-way ANOVA was used to determine statistical significane, and it was found that fold changes in samples incubated with nanoparticles of -23.52 mV, -15.6 mV and -4.4 mV were significantly different compared to whole blood without any nanoparticles added, while samples incubated with zymosan had a higher significant fold change.

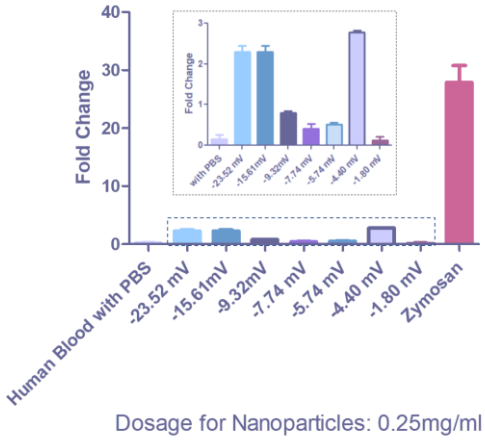

Figure 1. Fold change for C5a in human whole blood when incubated with nanoparticles of different zeta potential.

Conclusions: Preliminary experiments have shown that neutral nanoparticles having zeta potential of -1.80 mV result in lower fold change for the anaphylatoxin C5a when the nanoparticles are incubated with human whole blood in comparison to nanoparticles having zeta potential of -23.52 mV. Future work will be directed to further track the changes in other complement protein levels C3 and C3a and find how the complement protein levels will change in porcine whole blood, as pigs have a more spontaneous complement activation compared to humans.

References:

Szebeni, J. (2014). Complement activation-related pseudoallergy: a stress reaction in blood triggered by nanomedicines and biologicals. Molecular immunology, 61(2), 163-173.

Markiewski, M. M., & Lambris, J. D. (2007). The role of complement in inflammatory diseases from behind the scenes into the spotlight. The American journal of pathology, 171(3), 715-727.

Chonn, A., Cullis, P. R., & Devine, D. V. (1991). The role of surface charge in the activation of the classical and alternative pathways of complement by liposomes. The Journal of immunology, 146(12), 4234-4241.

Connor, E. F., Nyce, G. W., Myers, M., Möck, A., & Hedrick, J. L. (2002). First example of N-heterocyclic carbenes as catalysts for living polymerization: Organocatalytic ring-opening polymerization of cyclic esters. Journal of the American Chemical Society. https://doi.org/10.1021/ja0173324

Developing a Clinically Available Measure of Mucus Microrheology

Robert Hawkins, Katherine Joyner, Gregg Duncan.
Fischell Department of Bioengineering, University of Maryland, College Park

Statement of Purpose: Clinicians currently rely on the indirect measures of spirometry and disease symptoms to evaluate patients with chronic obstructive lung diseases such as asthma, cystic fibrosis (CF), and chronic obstructive pulmonary disease (COPD). Previous studies attempting to detect more direct biomarkers have shown that the translational diffusion rate of polyethylene glycol (PEG) coated muco-inert nanoparticles (MIP) is correlated with increases in total solids content and viscoelasticity of mucus samples produced from patients with CF, but the required technology is not available in clinical laboratories[1]. Here, we show that the rotational diffusion of MIP, as measured by fluorescence polarization (FP) using pre-existing technology found in clinical laboratories, is interdependent with MIP translational diffusion and as a result, correlated with mucus microrheology. The rotational diffusion of MIP was found to be correlated with the mucin concentration and the corresponding translational diffusion rate of MIP in an *in vitro* mucosal-mimic hydrogel model. Additionally, from rotational diffusion measurements, the bulk viscosity of glycerol, a well characterized solution, was able to be accurately estimated. Collectively, these findings suggest the potential for the rotational diffusion rate of MIP, as measured by FP, to act as a clinically-available measure of disease status and progression for obstructive lung diseases.

Methods: Muco-inert nanoparticles (MIP) were formulated by coating fluorescent 100nm and 500nm polystyrene nanoparticles with a high surface density of polyethylene glycol (PEG; Creative PEGWorks). The translational diffusion of MIP was measured by tracking the mean squared-displacement of individual nanoparticles at 30 frames/sec for 10 seconds using fluorescence video microscopy and multiple particle tracking (MPT). The rotational diffusion of MIP was measured using fluorescence polarization (FP) with excitation/emission wavelengths of 530/590. A mucus hydrogel model was constructed by mixing varying w/v concentrations of porcine gastric mucin (PGM; Sigma-Aldrich) with 2% w/v 4-arm PEG-thiol (PEG-4SH; 10 kDa).

Results: The rotational diffusion of both 100nm and 500nm MIP was found to decrease with increasing mucin concentration in 1-5% PGM/2% PEG-4SH w/v mucus hydrogel models and displayed a high degree of sensitivity in differentiating between consecutive concentration steps (Figure 1). The rotational diffusion of 100nm and 500nm MIP was also found to be strongly correlated with MIP translational diffusion in 1-5% PGM/2% PEG-4SH w/v mucus hydrogel models (Figure 2). As the translational diffusion decreased in 100nm and 500nm MIP, the rotational diffusion of the corresponding MIP also decreased. Lastly, the bulk viscosity of 0-100% w/v glycerol solutions were able to be accurately estimated using the rotational diffusion values of 100nm and 500nm MIP obtained through FP (Figure 3).

Conclusions: The ability to effectively measure microrheology using rotational diffusion of muco-inert nanoparticles (MIP) was explored using fluorescence polarization (FP). The rotational diffusion of 100nm and 500nm muco-inert nanoparticles (MIP) was found to be correlated with increasing mucin concentrations in a mucus hydrogel model. Mucin concentration is a known biomarker of chronic obstructive lung diseases and so these findings suggest the potential for the rotational diffusion of MIP to be used to monitor disease status and progression in patients. The rotational diffusion of MIP was also found to be correlated with the corresponding MIP translational diffusion. As the translational diffusion of MIP is a previously validated measure of microrheology, these results indicate that the rotational and translational diffusion of MIP are interdependent and as a result, indicate that the rotational diffusion of MIP is correlated with mucus microrheology. Additionally, using the rotational diffusion of MIP, the viscosities of various concentrations of glycerol were able to be accurately estimated. This ability indicates potential for the rotational diffusion of MIP to be used to produce physiologically-relevant estimates of patient mucus viscosity. Importantly, the ability to accurately measure the rotational diffusion of MIP using FP will allow this procedure to be readily performed in a clinical setting as FP is already used to perform immunoassays in blood, urine, and other biological samples in clinical laboratories[2].

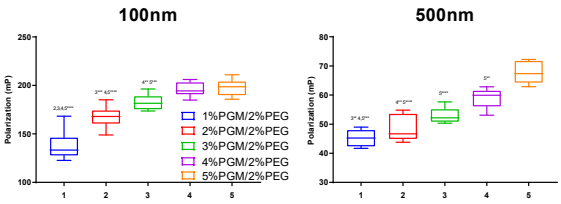

Figure 1. Rotational diffusion of 100nm and 500nm MIP in 1-5% porcine gastric mucin (PGM) with 2% 4-arm PEG-SH.

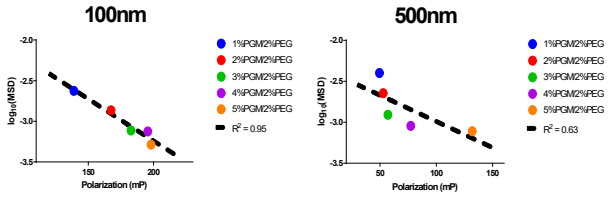

Figure 2. Rotational diffusion and $\log_{10}$(MSD) of 100nm and 500nm MIP in 1-5% PGM/ 2% 4-arm PEG-SH.

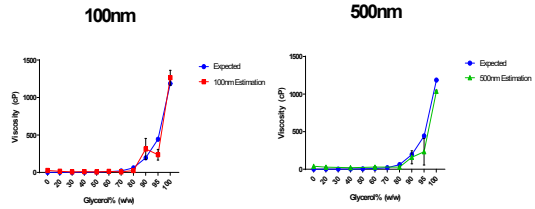

Figure 3. Estimation of viscosity of 0-100% w/w glycerol solutions based on 100nm and 500nm MIP rotational diffusion.

References:
1. Duncan et al. (2016). Microstructural alterations of sputum in cystic fibrosis lung disease. *JCI Insight,* 1(18):e88198
2. Tagit, O., & Hildebrandt, N. (2016). Fluorescence Sensing of Circulating Diagnostic Biomarkers Using Molecular Probes and Nanoparticles. *ACS Sensors, 2*(1), 31-45

Engineering Bispecific Antibodies to Synergistically Inhibit Tumor Metastasis

Yun-Huai Kuo[1], Huilin Yang[1], Wentao Wang[2], A.J. Cariaga[1], Jamie Spangler[1,2].
[1]Department of Chemical and Biomolecular Engineering, [2]Department of Biomedical Engineering, Johns Hopkins University

Statement of Purpose:

Metastasis is responsible for 90% of deaths from solid tumors. While most current cancer treatments focus on controlling tumor proliferation, the mechanisms behind cancer metastasis have yet to be fully elucidated. Recently, an interleukin-6 (IL-6)/interleukin-8 (IL-8) synergistic signaling pathway was found to be responsible for cancer cell migrations. Inhibition of IL-6 and IL-8 receptors (IL-6R and IL-8R) can effectively reduce metastasis, revealing a promising therapeutic strategy to decrease the metastatic capability of cancer cells. Recombinant bispecific antibodies have high specificity, affinity, potency, and avidity. They also have less risk of secondary resistance caused by mutational escape. Utilizing this attractive antibody platform, we engineered recombinant bispecific antibodies that can simultaneously target and inhibit both IL-6R and IL-8R. Our bispecific antibodies have shown significant efficacy in reducing cancer cell motility. We are measuring the binding affinity and investigating the inhibitory effects of our bispecific antibodies compared to commercially available monospecific antibodies to further characterize their therapeutic effects. Effectively suppressing cancer metastasis with our bispecific antibody constructs could be a monumental step in drastically improving patient outcomes.

Methods:

Single-chain variable fragments (scFVs) of the commercial anti-IL-6R antibody Tocilizumab and the anti-IL-8R antibody 10H2 were used to generate bispecific antibodies of various configurations. Of all the variants generated, only two, BS1 and BS2, were able to be expressed in HEK293 cells.

To determine the binding affinities of the two bispecific constructs compared to Tocilizumab and 10H2, binding studies were performed using a triple negative breast cancer cell line, MDA-MB-231, and a fibrosarcoma cell line, HT1080. The degree of binding was assessed through flow cytometry.

A surface receptor staining assay was conducted for oral keratinocytes, a potential cell line useful for further characterization of the bispecific constructs in order to determine IL-6R and IL-8R surface expression.

The binding of the bispecific constructs with IL-6R was further compared with Tocilizumab and 10H2 using bio-layer inferometry.

Tumor cell migration studies were performed to investigate the ability of the bispecific constructs to inhibit tumor migration. MDA-MB-231 cells and HT1080 cells were cultured in 3D collagen I matrices. Following treatment, individual cells were tracked, and their motility

Results:

Large scale expression and purification of BS1 and BS2 in HEK293 cells yielded 1.6-3mg and 0.5mg of protein per liter of supernatant.

Binding studies using MDA-MB-231 cells showed that BS1 had a binding affinity with MDA-MB-231 cells of 28.6 nM, and BS2 had a kD of 6.95 nM, while 10H2 had a kD of 248 nM, and Tocilizumab did not appear to bind.

The surface receptor staining assay identified the concurrent expression of IL-6R and IL-8R on oral keratinocyte cells, confirming their utility for further characterization of the bispecific constructs.

When assessed with bio-layer inferometry for binding to IL-6R, the bivalent Tocilizumab showed a kD of 31 nM, comparable to that of the bivalent BS2 75 nM, while the monovalent BS1 had a lower kD of 120 nM. As expected, 10H2 did not bind to IL-6R.

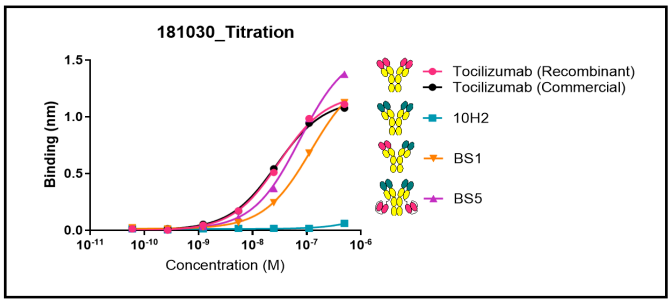

Figure 1. Binding Affinities to IL-6R measured by bio-layer inferometry

3D tumor cell migration studies showed that both BS1 and BS2 effectively inhibit tumor cell migration.

Conclusions:

We were able to design and produce recombinant bispecific antibodies and have shown that they bind to IL-6R and IL-8R with higher affinities than Tocilizumab and 10H2 monoclonal antibodies. Additionally, we have shown that the bispecific constructs are more effective than the combination of Tocilizumab and 10H2 in inhibiting the migration of highly motile tumor cells. These results are tremendously promising and prove that targeting the synergistic IL-6 and IL-8 pathways with bispecific antibodies could be an effective strategy to inhibit tumor metastasis.

For the future, further characterization of the bispecific constructs using oral keratinocytes would elucidate the avidity effect thereof. It would also be crucial to assess the competitive inhibition of IL-6 and IL-8 signaling pathways with the bispecific constructs, thereby further identifying the inhibitory effects thereof. Finally, it would be of great interest to introduce the bispecific constructs into mouse xenograft models to evaluate their ability to inhibit tumor metastasis *in vivo*.

References:

1. Jayatilaka, H. Nat Commun. 2017; 8
2. Chaffer, CL. Science. 2011; 331
3. Chuntharapai, A. J Immunol. 1994; 153